

RESEARCH PAPER

## Synthesis and Nanostructure Characterization of Azo-Polymer, Modified with Trichloroethylene, Containing Metal-Oxide Nanoparticles for Improved Optoelectronic Properties

Nawar Jamal Abdulrada <sup>1\*</sup>, Mohammed Ali Mutar <sup>2</sup>

<sup>1</sup> Department of Chemistry, College of Education for Pure Science (Ibn Al- Haitham), University of Baghdad, Baghdad, Iraq

<sup>2</sup> Department of Chemistry, College of Sciences, University of AL-Qadisiyah, Iraq

### ARTICLE INFO

#### Article History:

Received 11 December 2025

Accepted 15 February 2026

Published 01 April 2025

#### Keywords:

Modified Pechini method

Nanostructure

TiO<sub>2</sub>

XRD analysis

ZnO

### ABSTRACT

This research article discusses the preparation of metal-oxide nanoparticles, namely, TiO<sub>2</sub> and ZnO, through a modified Pechini method, in which citric acid was employed as fuel and capping agent. To determine the TiO<sub>2</sub> and ZnO nanoparticles, a various analyses including X-ray Diffraction (XRD), Fourier Transform Infrared Spectroscopy (FTIR) and Field Emission Scanning Electron Microscopy (FESEM) was carried out. The XRD patterns confirmed that TiO<sub>2</sub> crystallizes in the anatase phase and ZnO crystallizes in the hexagonal wurtzite structure. Morphological analysis showed a homogeneous nanostructure of well dispersed particles with mean size of 94.22 nm for TiO<sub>2</sub> and 55.19 nm for ZnO. The results of structural and morphological clearly support a fact that structure stability and function performance in different applications is strongly supported by metal oxide's properties.

#### How to cite this article

Abdulrada N., Mutar M. *Synthesis and Nanostructure Characterization of Azo-Polymer, Modified with Trichloroethylene, Containing Metal-Oxide Nanoparticles for Improved Optoelectronic Properties*. J Nanostruct, 2026; 16(2):1538-1544. DOI: 10.22052/JNS.2026.02.005

### INTRODUCTION

Nanotechnology is an evolving sector of science and engineering that investigates the ability to manipulate and control the properties of materials at the nanoscale, between 1-100 nm [1, 2]. Nanosized materials exhibit distinctly different behaviors than bulk-scale substances. The reason for this lies in extensive surface exposure, quantum effects, and altered atomic/electronic structures [3]. Nanomaterials have been greatly studied, with metal oxide being one of the most

studied types of this category. Nano-sized metal oxides possess a wide range of properties, they demonstrate high structural strength, and are applicable in numerous ways [4]. Employing the nano-science can effectively improve the physico-chemical properties of metal oxides, making them promising in a wide range of applications such as catalysis [5], energy storage [6], environmental protection [6], and biomedical engineering [7]. The increase in the surface-to-volume ratio of metal oxides is one of the greatest benefits

\* Corresponding Author Email: [nawar.j.ar@ihcoedu.uobaghdad.edu.iq](mailto:nawar.j.ar@ihcoedu.uobaghdad.edu.iq)

of nanotechnology. In bulk metal oxides, the majority of the atoms are located inside the bulk structure; however, in metal oxide nanoparticles, a large percentage of the atoms are located on the surface [8]. This increase in surface area has a strong effect on the physical properties of metal oxides, including: electrical conductivity, thermal conductivity, optical absorption, and mechanical strength [9, 10]. For example; nano-metal oxides such as  $\text{TiO}_2$  and  $\text{ZnO}$  showed improved optical properties against their bulk states, offering the great transparency and absorption of light, which can be an option for photocatalytic and photovoltaic devices [11-13]. The morphology and crystal structures of metal oxides are major factors in altering their physical behavior [14]. To date, a series of nano-metal oxides having different morphologies including nanoparticles, nanowires, nanotubes, nanosheets and thin films have been achieved through employing different advanced synthesis techniques such as sol-gel processing, hydrothermal, co-precipitation, sonochemical and chemical vapour deposition [15, 16]. The morphological characteristics of metal oxides impact the electrochemical properties in lithium-ion batteries [17, 18], supercapacitors [19], and photoelectrochemical cells [20]. Nanotechnology not only affects the physical attributes of metal oxides; but also it has a very strong effect on their chemical attributes. Of all the metal oxide nanomaterials that researchers have investigated,  $\text{ZnO}$  and  $\text{TiO}_2$  are particularly prominent. Due to their excellent chemical stability and tunable electronic properties, these compounds have been used in photocatalysis [21, 22], sensors [23, 24], energy storage devices [25, 26], and biomedical applications [27, 28]. Although both are wide-bandgap semiconductors, they have very different phase behavior, structural characteristics, and morphology-dependent properties that impact their performance for different applications. The hexagonal wurtzite structure (space group P63mc) is the only naturally occurring form of  $\text{ZnO}$  and is the most stable crystal phase under standard conditions [29]. Previous studies indicated that alternative crystal forms (e.g., cubic zinc blende and cubic rocksalt  $\text{ZnO}$ ) can be produced under extreme synthesis conditions; however, these other phases of  $\text{ZnO}$  are typically metastable and not common [30]. On the other hand,  $\text{TiO}_2$  exists in three main types of crystal structures: anatase, rutile, and brookite. Of these, anatase and rutile

are the two most commonly studied and used for many applications [31]. Anatase has a tetragonal structure (I41/amd) with distortions of the  $[\text{TiO}_6]$  octahedra. Rutile with tetragonal structure (P42/mnm) is the densest of the three forms. Rutile is also the thermodynamically stable form of  $\text{TiO}_2$  and is found as larger size crystals and produced at higher temperatures [32]. Although brookite has an orthorhombic structure (Pbca) and is a metastable form, it is a very rare form of  $\text{TiO}_2$  produced in synthesis reactions [33]. The relative stability of the three forms of  $\text{TiO}_2$  and what phase transitions occur between them will depend greatly on several factors, including synthesis method, temperature of synthesis, and size of particles.  $\text{ZnO}$  and  $\text{TiO}_2$  can produce multiple types of morphologies such as nanoparticles, nanorods, nanowires, nanosheets, nanotubes, and hierarchical/porous structures. The surface area value, exposed facets, defect density and charge transport pathways are key factors that affect by morphological characteristics of nano-metal oxides. Although  $\text{ZnO}$  and  $\text{TiO}_2$  exhibit similar basic characteristics as wide bandgap semiconductor materials, they can differ with respect to their bandgap energy and their degree of excitonic binding.  $\text{ZnO}$  has a bandgap of  $\sim 3.37$  eV with an associated excitonic binding energy of  $\sim 60$  meV [34]. As a result,  $\text{ZnO}$  can be used as a UV emitter, laser diode and as a transparent conducting oxide [35-37]. The reports showed bandgap energies of  $\sim 3.2$  eV for anatase phase and  $\sim 3.0$  eV for rutile phase of  $\text{TiO}_2$  as an effective UV absorber. Anatase phase generally shows superior photocatalytic activity due to high charge separation and slow recombination rates of photogenerated electron-hole pairs [38]. To design and optimize the nanomaterials as high-performance compounds, it is important to understand how the crystal structure, morphology, and surface reactivity can all influence each other. In this paper we report the crystal phases, structural, and morphological features of  $\text{ZnO}$  and  $\text{TiO}_2$  nanostructures prepared via citric acid-assisted pechini method.

## MATERIALS AND METHODS

### Materials

For synthesis of  $\text{ZnO}$  and  $\text{TiO}_2$  nanoparticles, zinc nitrate hexahydrate ( $\text{Zn}(\text{NO}_3)_2 \cdot 6\text{H}_2\text{O}$ ), ethylene glycol ( $\text{C}_2\text{H}_6\text{O}_2$ ), citric acid ( $\text{C}_6\text{H}_7\text{O}_8$ ), ethanol ( $\text{C}_2\text{H}_5\text{OH}$ ) and titanium IV isopropoxide ( $\text{Ti}[\text{OCH}(\text{CH}_3)_2]_4$ ) were achieved from Merck

company.

#### Synthesis of ZnO nanostructures

To synthesize the ZnO nanostructures, the role of citric acid and ethylene glycol as chelating and polymerizing agents in pechini reaction was examined, respectively. Adjusting the molar ratio of 1:1 for citric acid:ethylene glycol and 3:1 for citric acid: Zn metal allowed for good chelation and a homogeneous metal ion distribution. In this reaction, the certain amount of Zn precursor was first dissolved in distilled water under stirring. A solution from citric acid was added to the above Zn solution to generate Zn-citrate complex. After that, polymerizing agent was introduced and a polyesterification reaction was occurred. The mixture was then heated at 120 °C for 2 h to allow evaporation of the solvent. Finally, the formed gel was dried at 65 °C for 18 h and then calcined

at 500 °C for 2h, resulting in complete removal of organic material, resulting in crystalline ZnO nanoparticles.

#### Synthesis of TiO<sub>2</sub> nanostructures

TiO<sub>2</sub> nanoparticles were fabricated *via* a modified Pechini technique with citric acid serving as a chelating agent and ethylene glycol functioning as a polymerizing agent; a molar ratio of 1:1 for citric acid to ethylene glycol was used, while retaining a molar ratio of 3:1 for citric acid: Ti ion for optimum chelation and uniformity of metal species distribution. Ethanol was served as the solvent for the reaction. To begin the synthesis, the citric acid and ethanol were mixed together under a magnetic stirrer until a clear and homogeneous solution was produced. When the citric acid was completely solubilized, the Ti precursor was added to the solution at a controlled rate in order

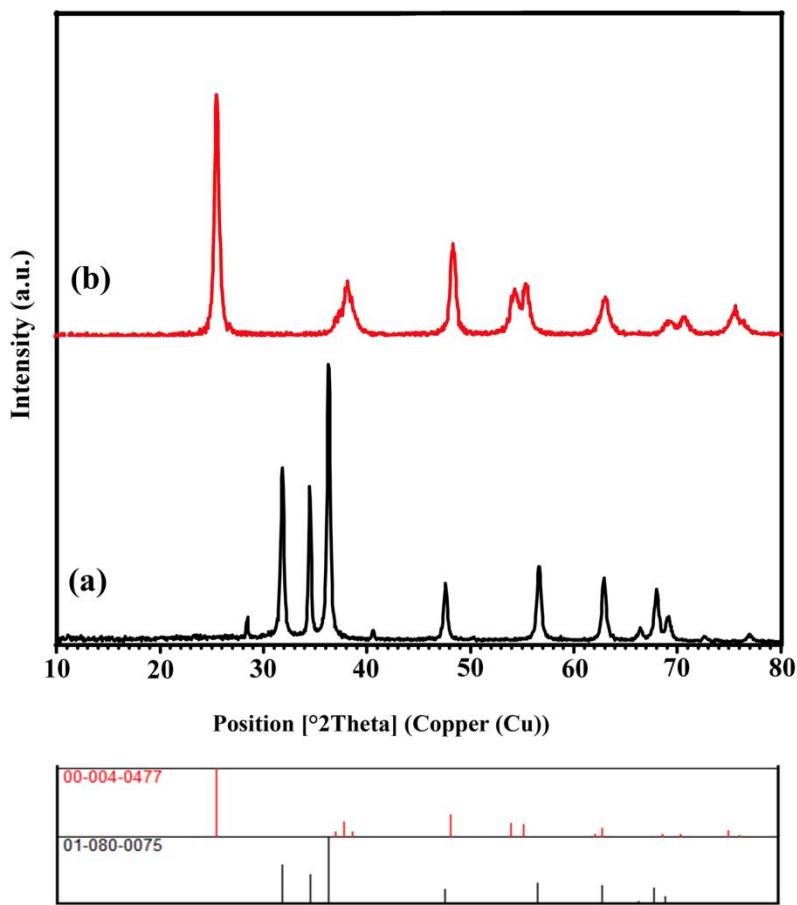


Fig. 1. XRD patterns of pechini synthesized (a) ZnO and (b) TiO<sub>2</sub> nanoparticles

to achieve the maximum amount of interaction between Ti ions and citric acid. After that, ethylene glycol was added slowly as the final component to trigger the polyesterification reaction, resulting in the development of a polymeric network. The formed sol was subsequently exposed to heat for solvent evaporation as well as polymerization. This sol was converted into a gel. The resulting gel was dried at 50 °C for 18 h and then underwent heat treatment to remove organic substrates within the gel and to produce crystallized  $\text{TiO}_2$  nanocrystals at 400 °C for 2 h.

#### Characterization methods

For evaluation of the crystalline structure and phase composition of  $\text{ZnO}$  and  $\text{TiO}_2$  nanoparticles, X-ray diffraction (XRD, Philips-X'Pert-Pro – monochromatized  $\text{Cu K}\alpha$  radiation;  $\lambda=1.54\text{\AA}$ ) was employed. The fabricated nano-metal oxides were identified through Fourier transform infrared (FT-IR, Nicolet Magna- 550 spectrophotometer)

to illustrate the functional groups of samples. Furthermore, Field emission scanning electron microscopy (FE-SEM, MIRA3 TESCAN) was followed for analyzing the morphological properties of samples.

#### RESULTS AND DISCUSSION

According to the XRD result of the  $\text{ZnO}$  nanostructures in Fig. 1a, the high-intensity peaks confirm its excellent crystalline quality. The characteristic peaks found at approximately 31.7°, 34.4°, 36.2°, 47.5°, 56.6°, 62.8°, and 67.9° correspond to the (100), (002), (101), (102), (110), (103), and (112) planes, respectively, of hexagonal wurtzite-type  $\text{ZnO}$  as defined in standard JCPDS data (01-080-0075). The comparatively intense (100), (002), and (101) peaks point to the fact that there is a preference for preferential growth of the crystals in particular directions of crystalline  $\text{ZnO}$  structure. The XRD pattern of the  $\text{TiO}_2$  nanostructures in Fig. 1b indicates good

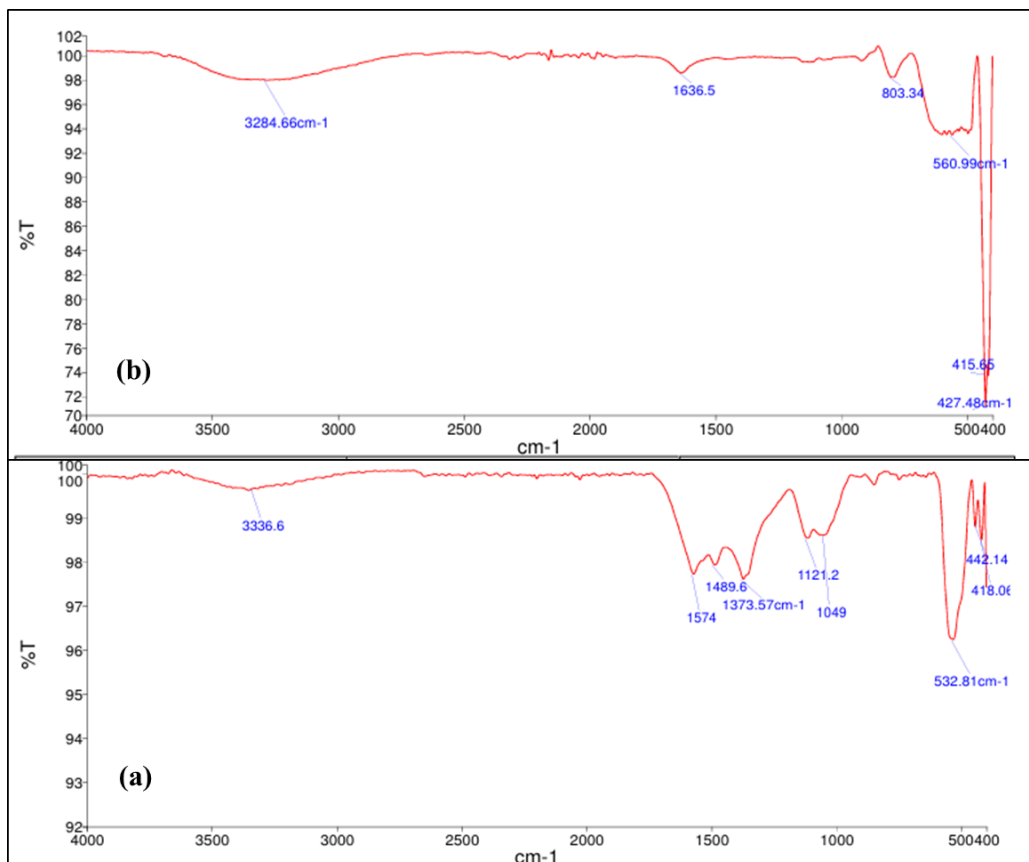


Fig. 2. FTIR spectra of (a)  $\text{ZnO}$  and (b)  $\text{TiO}_2$  nanoparticles synthesized via citric acid-assisted reaction.

crystallinity due to the presence of distinct peaks. Various major peaks located at around  $25.3^\circ$ ,  $37.8^\circ$ ,  $48.0^\circ$ ,  $54.0^\circ$ ,  $55.1^\circ$ ,  $62.7^\circ$ ,  $68.6^\circ$ ,  $70.3^\circ$ , and  $75.0^\circ$  correspond to peaks found in the standard JCPDS data (00-004-0477) that belong to crystallographic planes (101), (004), (200), (105), (211), (204), (116), (220), and (215) of the anatase  $\text{TiO}_2$  phase. The dominant crystalline structure is anatase as indicated by the strong (101) peak at around  $25.3^\circ$  and no additional diffraction peaks indicating the presence of rutile or brookite. Therefore it can be seen that pure-phase  $\text{TiO}_2$  (anatase) was successfully synthesized using the Pechini method.

The FTIR spectrum of  $\text{ZnO}$  nanoparticles in Fig. 2a shows broad peaks at  $3000\text{-}3600\text{ cm}^{-1}$  due to the residual water on the surface of  $\text{ZnO}$  (stretching vibration). The absorption band at  $1640\text{ cm}^{-1}$  indicates the presence of H-O-H groups (bending vibration). The strong peaks ranging from  $400$  to  $550\text{ cm}^{-1}$  corresponds to the  $\text{Zn}-\text{O}$

bond's stretching vibration, demonstrating the successful formation of  $\text{ZnO}$  nanostructures. Also, it should be noted that the observed peaks within  $1000\text{-}1500\text{ cm}^{-1}$  may be related to the organic templates and asymmetric stretching vibration of nitrate ions [39, 40]. In the FTIR spectrum of  $\text{TiO}_2$  nanoparticles (Fig. 2b), there is a broad peak in the region of  $3000\text{-}3600\text{ cm}^{-1}$ , which represents the stretching vibrations of  $-\text{OH}$  due to physically adsorbed water. In addition, there is weak peak due to the bending vibration of  $\text{H}-\text{O}-\text{H}$ , which occurs at  $1636\text{ cm}^{-1}$ . The most important features of the  $\text{TiO}_2$ 's FTIR spectrum were below  $800\text{ cm}^{-1}$  and corresponded to metal-oxygen vibrations. The absorption peaks, between  $400$  and  $700\text{ cm}^{-1}$ , can be assigned to the  $\text{Ti}-\text{O}$  or  $\text{Ti}-\text{O}-\text{Ti}$  stretching of the  $\text{TiO}_2$  lattice. Furthermore, the absence of peaks associated with organic functional groups implied that no organic residues remained after calcination of the nanomaterials [41].

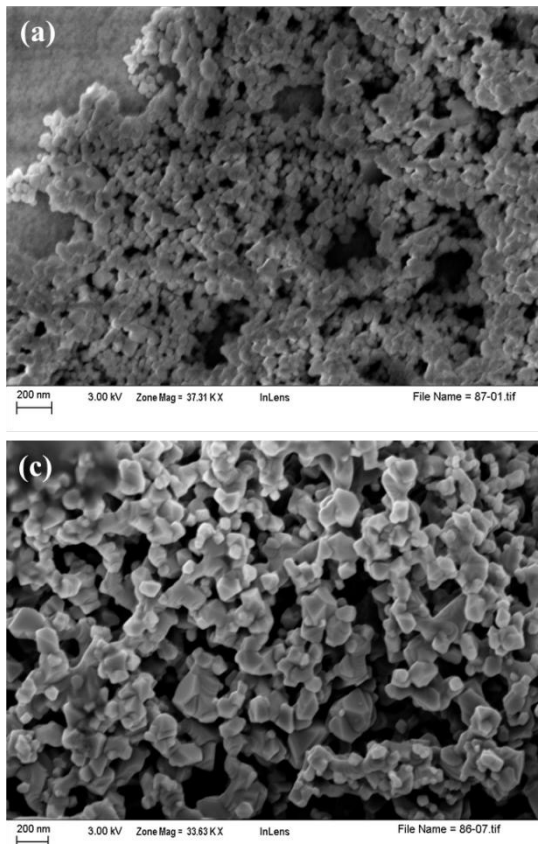
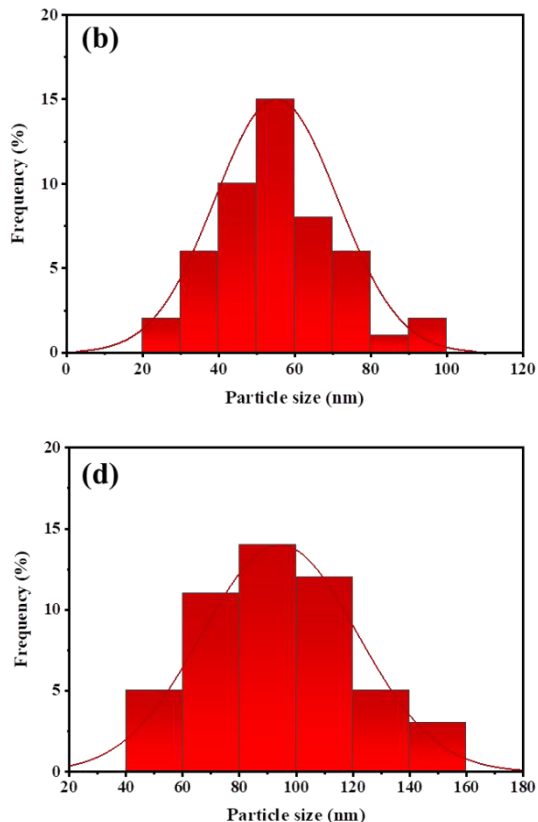


Fig. 3. FESEM images and particle size distribution plots of (a, b)  $\text{ZnO}$  and (c, d)  $\text{TiO}_2$  nanoparticles synthesized via citric acid-assisted reaction.



The ZnO nanoparticle's uniformity is extremely high. In FESEM image and particle size distribution plot of Fig. 3(a, b), the ZnO nanoparticles are spherical having narrow size distributions. The uniformity of shape and particle size indicates that the nanoparticles grow orderly. In some cases, slight clustering was found. A homogeneous precursor solution creates conditions to prevent uncontrolled nanocrystal growth and possess similar sizes and shapes. These results support the Pechini method as a reliable way to produce high-quality nanostructures with controlled shape. Morphological uniformity can improve their performance in catalytic, optical, and electronic applications.

The FESEM image and particle size distribution plot of  $\text{TiO}_2$  structures in Fig. 3(c, d) show the distribution of nanoparticles is uniform and there is a homogeneous distribution in the sample. The majority of these nanoparticles is quasi-spherical in shape and has the same size, indicating how the Pechini process can control the nucleation and growth phase of  $\text{TiO}_2$  nanoscale structures. Variations in the  $\text{TiO}_2$  nanoparticle's size confirm the strong interaction between Ti ions and the polymeric precursor matrix. This level of synthetic uniformity ensures that synthesized  $\text{TiO}_2$  nanoparticles have a high degree of morphological uniformity, which is essential for applications in which the uniformity of the surface area and active sites on materials is important.

## CONCLUSION

In summary, the single phased metal oxide nanostructures, including ZnO and  $\text{TiO}_2$ , were rationally designed via modified pechini method. In the synthesis reaction, role of citric acid as a chelating or capping agent and role of ethylene glycol as polymerizing agent was followed in formation of homogenous oxide powder. XRD patterns validated the hexagonal wurtzite for ZnO and anatase phase for  $\text{TiO}_2$  structures. Observation data from FESEM analysis showed that quasi-spherical and well-dispersed particles were formed for both ZnO and  $\text{TiO}_2$  nanoparticles, describing the mean particle size of 55.19 nm and 94.22 nm, respectively. Homogeneous nucleation and controlled growth kinetics in pechini synthesis method resulted from metal (Ti and Zn)-citrate complexes and a polymeric network with ethylene glycol. These structural and morphological features can provide high-quality ZnO and  $\text{TiO}_2$

nanoparticles with effective efficiency in different catalytic and energetic fields.

## ACKNOWLEDGEMENTS

The authors thank the Department of Chemistry, University of Baghdad and College of Sciences, University of Al-Qadisiyah for laboratory facilities and technical support during this work.

## CONFLICT OF INTEREST

The authors declare that there is no conflict of interests regarding the publication of this manuscript.

## REFERENCES

1. Malik S, Muhammad K, Waheed Y. Nanotechnology: A Revolution in Modern Industry. *Molecules*. 2023;28(2):661.
2. Logothetidis S. *Nanotechnology: Principles and Applications*. NanoScience and Technology: Springer Berlin Heidelberg; 2011. p. 1-22.
3. Fernández-García M, Martínez-Arias A, Hanson JC, Rodriguez JA. *Nanostructured Oxides in Chemistry: Characterization and Properties*. *Chem Rev*. 2004;104(9):4063-4104.
4. Gajewicz A, Puzyn T, Rasulev B, Leszczynska D, Leszczynski J. *Metal Oxide Nanoparticles: Size-Dependence of Quantum-Mechanical Properties*. *Nanoscience and Nanotechnology-Asia*. 2012;1(1):53-58.
5. Sharma RK, Bandichhor R, Mishra V, Sharma S, Yadav S, Mehta S, et al. Advanced metal oxide-based nanocatalysts for the oxidative synthesis of fine chemicals. *Materials Advances*. 2023;4(8):1795-1830.
6. Yaqoob AA, Ahmad A, Ibrahim MNM, Karri RR, Rashid M, Ahamad Z. *Synthesis of metal oxide-based nanocomposites for energy storage application*. Sustainable Nanotechnology for Environmental Remediation: Elsevier; 2022. p. 611-635.
7. Andreeescu S, Ornatska M, Erlichman JS, Estevez A, Leiter JC. *Biomedical Applications of Metal Oxide Nanoparticles. Fine Particles in Medicine and Pharmacy*: Springer US; 2011. p. 57-100.
8. Lien D-H, Durán Retamal JR, Ke J-J, Kang C-F, He J-H. Surface effects in metal oxide-based nanodevices. *Nanoscale*. 2015;7(47):19874-19884.
9. Rahman MT, Hoque MA, Rahman GT, Gafur MA, Khan RA, Hossain MK. Evaluation of thermal, mechanical, electrical and optical properties of metal-oxide dispersed HDPE nanocomposites. *Materials Research Express*. 2019;6(8):085092.
10. Chavali MS, Nikolova MP. Metal oxide nanoparticles and their applications in nanotechnology. *SN Applied Sciences*. 2019;1(6).
11. He H, Liu C, Dubois KD, Jin T, Louis ME, Li G. Enhanced Charge Separation in Nanostructured  $\text{TiO}_2$  Materials for Photocatalytic and Photovoltaic Applications. *Industrial and Engineering Chemistry Research*. 2012;51(37):11841-11849.
12. Chen X, Wu Z, Liu D, Gao Z. Preparation of ZnO Photocatalyst for the Efficient and Rapid Photocatalytic Degradation of Azo Dyes. *Nanoscale Research Letters*. 2017;12(1).
13. Cembrero J. Nanocolumnar ZnO films for photovoltaic

applications. *Thin Solid Films*. 2004;451-452:198-202.

14. Korotcenkov G. The role of morphology and crystallographic structure of metal oxides in response of conductometric-type gas sensors. *Materials Science and Engineering: R: Reports*. 2008;61(1-6):1-39.

15. Yadav S, Rani N, Saini K. A review on transition metal oxides based nanocomposites, their synthesis techniques, different morphologies and potential applications. *IOP Conference Series: Materials Science and Engineering*. 2022;1225(1):012004.

16. Guo T, Yao M-S, Lin Y-H, Nan C-W. A comprehensive review on synthesis methods for transition-metal oxide nanostructures. *CrystEngComm*. 2015;17(19):3551-3585.

17. Wu HB, Chen JS, Hng HH, Wen Lou X. Nanostructured metal oxide-based materials as advanced anodes for lithium-ion batteries. *Nanoscale*. 2012;4(8):2526.

18. Wang L, Yue S, Zhang Q, Zhang Y, Li YR, Lewis CS, et al. Morphological and Chemical Tuning of High-Energy-Density Metal Oxides for Lithium Ion Battery Electrode Applications. *ACS Energy Letters*. 2017;2(6):1465-1478.

19. Ma Y, Xie X, Yang W, Yu Z, Sun X, Zhang Y, et al. Recent advances in transition metal oxides with different dimensions as electrodes for high-performance supercapacitors. *Advanced Composites and Hybrid Materials*. 2021;4(4):906-924.

20. Yang Y, Niu S, Han D, Liu T, Wang G, Li Y. Progress in Developing Metal Oxide Nanomaterials for Photoelectrochemical Water Splitting. *Advanced Energy Materials*. 2017;7(19).

21. Hussain M, Ceccarelli R, Marchisio DL, Fino D, Russo N, Geobaldo F. Synthesis, characterization, and photocatalytic application of novel  $\text{TiO}_2$  nanoparticles. *Chem Eng J*. 2010;157(1):45-51.

22. Hong RY, Li JH, Chen LL, Liu DQ, Li HZ, Zheng Y, et al. Synthesis, surface modification and photocatalytic property of  $\text{ZnO}$  nanoparticles. *Powder Technol*. 2009;189(3):426-432.

23. Singh AK. Synthesis, characterization, electrical and sensing properties of  $\text{ZnO}$  nanoparticles. *Adv Powder Technol*. 2010;21(6):609-613.

24. Jasmin J, Anilkumar P, Deepak S. Synthesis, analysis and characterization of surfactant-assisted  $\text{TiO}_2$  nanoparticles for ammonia gas sensor applications. *Ceram Int*. 2024;50(24):52262-52269.

25. Sami S, Etesami N. Improving thermal characteristics and stability of phase change material containing  $\text{TiO}_2$  nanoparticles after thermal cycles for energy storage. *Appl Therm Eng*. 2017;124:346-352.

26. Kaur D, Sharma T, Madhu C. Dielectric investigations of pristine and modified  $\text{ZnO}$  nanoparticles for energy storage devices. *Journal of Materials Science: Materials in Electronics*. 2022;33(13):9905-9917.

27. Mirzaei H, Darroudi M. Zinc oxide nanoparticles: Biological synthesis and biomedical applications. *Ceram Int*. 2017;43(1):907-914.

28. Dessai S, Ayyanar M, Amalraj S, Khanal P, Vijayakumar S, Gurav N, et al. Bioflavonoid mediated synthesis of  $\text{TiO}_2$  nanoparticles: Characterization and their biomedical applications. *Mater Lett*. 2022;311:131639.

29. Barros BS, Barbosa R, dos Santos NR, Barros TS, Souza MA. Synthesis and x-ray diffraction characterization of nanocrystalline  $\text{ZnO}$  obtained by Pechini method. *Inorg Mater*. 2006;42(12):1348-1351.

30. Kuang F-G, Kuang X-Y, Kang S-Y, Zhong M-M, Sun X-W. Ab initio study on physical properties of wurtzite, zincblende, and rocksalt structures of zinc oxide using revised functionals. *Mater Sci Semicond Process*. 2015;31:700-708.

31. De Matteis V, Cascione M, Brunetti V, Toma CC, Rinaldi R. Toxicity assessment of anatase and rutile titanium dioxide nanoparticles: The role of degradation in different pH conditions and light exposure. *Toxicol In Vitro*. 2016;37:201-210.

32. Silva Junior E, La Porta FA, Liu MS, Andrés J, Varela JA, Longo E. A relationship between structural and electronic order-disorder effects and optical properties in crystalline  $\text{TiO}_2$  nanomaterials. *Dalton Transactions*. 2015;44(7):3159-3175.

33. Manzoli M, Freyria FS, Blangetti N, Bonelli B. Brookite, a sometimes under evaluated  $\text{TiO}_2$  polymorph. *RSC Advances*. 2022;12(6):3322-3334.

34. Mohammad AM, Ahmed Al-Jaf HS, Ahmed HS, Mohammed MM, Khodair ZT. Structural and morphological studies of  $\text{ZnO}$  nanostructures. *Journal of Ovonic Research*. 2022;18(3):443-452.

35. Kong YC, Yu DP, Zhang B, Fang W, Feng SQ. Ultraviolet-emitting  $\text{ZnO}$  nanowires synthesized by a physical vapor deposition approach. *Appl Phys Lett*. 2001;78(4):407-409.

36. Lee J-H, Ko K-H, Park B-O. Electrical and optical properties of  $\text{ZnO}$  transparent conducting films by the sol-gel method. *J Cryst Growth*. 2003;247(1-2):119-125.

37. Liang HK, Yu SF, Yang HY.  $\text{ZnO}$  random laser diode arrays for stable single-mode operation at high power. *Appl Phys Lett*. 2010;97(24).

38. Zhang J, Zhou P, Liu J, Yu J. New understanding of the difference of photocatalytic activity among anatase, rutile and brookite  $\text{TiO}_2$ . *Physical Chemistry Chemical Physics*. 2014;16(38):20382-20386.

39. Vandamar Poonguzhalai R, Ranjith Kumar E, Sumithra MG, Arunadevi N, Rahale CS, Munshi AM, et al. Natural citric acid (lemon juice) assisted synthesis of  $\text{ZnO}$  nanostructures: Evaluation of phase composition, morphology, optical and thermal properties. *Ceram Int*. 2021;47(16):23110-23115.

40. Shoja Razavi R, Reza Loghman-Estarki M, Farhadi-Khouzani M, Barekat M, Jamali H. Large Scale Synthesis of Zinc Oxide Nano- and Submicro-Structures by Pechini Method: Effect of Ethylene glycol/Citric Acid Mole Ratio on Structural and Optical Properties. *Current Nanoscience*. 2011;7(5):807-812.

41. Vargas-Urbano MA, Marín L, Castillo WM, Rodríguez LA, Magén C, Manotas-Albor M, et al. Effect of Ethylene Glycol: Citric Acid Molar Ratio and pH on the Morphology, Vibrational, Optical and Electronic Properties of  $\text{TiO}_2$  and  $\text{CuO}$  Powders Synthesized by Pechini Method. *Materials*. 2022;15(15):5266.